THE ASTROPHYSICAL JOURNAL, 398:441–453, 1992 October 20


# A STUDY OF THE VELOCITY FIELD IN THE LOCAL SUPERCLUSTER BASED ON A NEW PECULIAR-VELOCITY SAMPLE

KAZUHIRO SHIMASAKU AND SADANORI OKAMURA
Department of Astronomy, Faculty of Science, University of Tokyo, Bunkyo-ku, Tokyo 113, Japan
*Received 1991 November 11; accepted 1992 April 24*

## ABSTRACT

We study the velocity field in the Local Supercluster (LS) on the basis of a newly compiled data set of peculiar velocities of 306 spiral galaxies as well as two well-known samples by Aaronson et al. (194 spirals) and by Faber et al. (400 ellipticals). Our sample is the largest one of spiral galaxies available at present with distance estimates as good as those for the sample of Aaronson et al. Galaxy distances in our sample are determined in this study using the Tully-Fisher relation.

We apply to our sample and Aaronson et al.'s sample a slightly simplified version of the standard Great Attractor (GA) model and determine the model parameters by the identical procedures. These parameters are compared with those obtained by Faber & Burstein from the sample of Faber et al. using the standard GA model. We find a broad agreement in the model parameters. However, the direction of the GA is different by at most 26° among the three samples. The difference is significant in terms of the Local Anomaly, which is the perturbation in the nearby velocity field introduced in the standard GA model in order to explain the discrepancy between the observed and the predicted velocities of the Local Group (LG) with respect to the cosmic microwave background (CMB). The direction of the GA obtained from our sample is different from the direction of the LG motion with respect to the CMB by only 13° while the difference amounts to 37° and 38° for the samples of Aaronson et al. and Faber et al., respectively. Thus, the observed and the predicted motions of the LG agree reasonably well in our sample, unlike the other samples. This suggests that it is not necessary to invoke the Local Anomaly. Since the velocity field obtained from the three samples are consistent in the common region, the difference of the GA parameters is probably due to the difference of the sampling regions. This indicates that the standard GA model is too simple to delineate the detailed local peculiar velocity field and to discuss whether the Local Anomaly exists or not.

*Subject headings:* galaxies: clustering — galaxies: distances and redshifts

## 1. INTRODUCTION

Galaxies with recession velocities less than $\sim 3000$ km s$^{-1}$ constitute the Local Supercluster (LS) to which the Local Group (LG) belongs (e.g., de Vaucouleurs 1978; Yahil, Sandage, & Tammann 1980; Tully 1982). The most dominant structure in the LS is the Virgo Cluster, which is located in the center of the LS. Peculiar velocities $V_{\rm pec}$, i.e., velocity components other than Hubble expansion velocities $V_{\rm H}$, of galaxies in the LS were studied by several authors (e.g., de Vaucouleurs & Bollinger 1979; Yahil et al. 1980; Tonry & Davis 1981; Aaronson et al. 1982a). They consistently detected in the peculiar velocity field an infall pattern toward the Virgo Cluster with the infall velocity of 200–400 km s$^{-1}$ at the LG (see Davis & Peebles 1983 for a review). It was clear, however, that the Virgo infall could not explain completely the peculiar velocity of the LG of 600 km s$^{-1}$ with respect to the cosmic microwave background (CMB) (Lubin et al. 1985; Fixen, Cheng, & Wilkinson 1983) even if the uncertainty of the Virgo infall velocity at the LG was taken into account.

On the basis of peculiar velocites of 10 clusters up to $V_{\rm H} \sim$ 10,000 km s$^{-1}$, Aaronson et al. (1986) showed that the peculiar velocity of the LG could be interpreted as the vector sum of the Virgo infall velocity and the velocity of the LS as a whole toward the Hydra-Centaurus supercluster, the nearest supercluster to the LS (see also Tammann & Sandage 1985). However, Dressler et al. (1987a) claimed that elliptical galaxies with $V_{\rm H} \lesssim 6000$ km s$^{-1}$ including those in the Hydra-Centaurus supercluster appeared to participate in a large-scale streaming motion toward $(l, b) = (312°, 6°)$ (see also Collins, Joseph, & Robertson 1986), where $l$ and $b$ are Galactic longitude and latitude, respectively. This large-scale streaming motion has been the subject and the driving force of many subsequent studies (e.g., Lynden-Bell et al. 1988; Faber & Burstein 1988, hereafter FB).

The Great Attractor (GA) model, proposed by Lynden-Bell et al. (1988) and revised by FB, is a standard model that explains the observed peculiar velocity field in the volume of $V_{\rm H} \lesssim 8000$ km s$^{-1}$ by gravitational infalls due to the postulated GA and the Virgo Cluster. Observational data on which the GA model is based are (1) peculiar velocities of 400 elliptical galaxies by Faber et al. (1989, hereafter 7S sample) and (2) those of some 200 spiral galaxies by Aaronson et al. (1982b, hereafter A82G sample). These two samples are the most reliable and largest data sets available in peculiar-velocity studies. They are complementary in depth and in spatial resolution. The 7S includes galaxies with distances as far as $V_{\rm H} \sim 8000$ km s$^{-1}$, and it covers almost all the sky. Thus, the 7S is suitable for the determination of the global structure of the model such as the position of the GA. On the other hand, galaxies in the A82G are relatively near ($V_{\rm H} \lesssim 2000$ km s$^{-1}$); namely, most of them belong to the LS. The spatial resolution is, however, much higher for the A82G than the 7S. Accordingly, the A82G is suitable for studying the velocity field in the LS, in particular, in our neighborhood.

There are, however, some tantalizing problems with the GA model. First, the existence of the GA has not been completely

established. There are not sufficient galaxies seen in the GA region (e.g., Saunders et al. 1991) although there appears to be an aggregation of galaxies located at nearly the right position (Dressler 1988). Mathewson, Ford, & Buchorn (1992) estimated peculiar velocities of as many as $\sim 700$ spiral galaxies in the GA region, but they could not find the backside infall to the GA position in contrast to the claim by Dressler & Faber (1990) and Dressler, Faber, & Burstein (1991) based on their samples of elliptical and S0 galaxies. Second, it is shown from the analysis of *IRAS* galaxies and the optical dipole that galaxies as distant as the GA do not account for the motion of the LG with respect to the CMB (Yahil 1988; Lynden-Bell & Lahav 1988). A wide-field imaging survey of the GA region in the near-infrared would be the important first step to the demonstration of the existence of the GA because the major part of the GA is heavily obscured by dust in our Galaxy. Finally, the motion of nearby galaxies raises a problem in the framework of the GA model. The LG and its nearby galaxies within $V_H \sim 700$ km s$^{-1}$ move together to a direction significantly different from that predicted by the GA model (FB). They call this discrepancy between the observed and predicted velocities of nearby galaxies the Local Anomaly (LA) and advocate that a nearby fluctuation of the mass density, for example, the postulated Local Void (Tully & Fisher 1987), induces the LA. However, the cause of the LA has not been identified yet.

Recently, a new surface photometric database of galaxies called Photometric Atlas of Northern Bright Galaxies (PANBG) was compiled at Kiso Observatory (Kodaira, Okamura, & Ichikawa 1990). The data base contains photometric parameters as well as images, isophotes, and profiles of 791 galaxies in the Revised Shapley-Ames Catalog of Bright Galaxies (Sandage & Tammann 1981, hereafter RSA). The PANBG has enabled us to make a new independent sample of peculiar velocities of galaxies in the LS which is larger than the A82G. In this paper, we analyze the peculiar velocity field in the LS on the basis of the new sample. The depth of the present sample is shallower than those of the 7S. Accordingly, it is irrelevant to ask whether the GA exists or not on the basis of the present sample. However, as in the case of the A82G, the present sample is more suitable for studying the velocity field in the LS than the 7S since it has a higher spatial resolution.

The structure of this paper is as follows. We define the new peculiar-velocity sample in § 2. Section 3 presents a qualitative overview of the velocity field of the LS based on the new sample. We examine in § 4 the global motion of LS galaxies quantitatively by using the slightly simplified GA model and discuss the significance of the LA; in other words, whether or not the systematic motion of the galaxies in the vicinity of the LG is significantly different from the global motion of LS galaxies as a whole. We also check the consistency among the samples in § 4. The conclusions are given in § 5.

## 2. THE NEW SAMPLE OF PECULIAR VELOCITIES

We make a new sample of peculiar velocities of 306 spiral galaxies in the LS, which is hereafter called the K90 sample. The reason for using spiral galaxies is that they are distributed more uniformly in space than ellipticals and therefore they are more suitable for studying the velocity field in detail.

In order to estimate the peculiar velocity of a galaxy, we have to measure its distance. The luminosity–line width relation (Tully & Fisher 1977, hereafter TF relation) is used to determine distances. The TF relation is generally supposed to be the most reliable distance indicator relation for spirals. The parameters necessary to construct the TF relation are total magnitudes, axial ratios, and H I 21 cm line widths. Axial ratios are used to calculate inclinations.

### 2.1. *Basic Data*

The photometric data, namely total magnitudes and axial ratios at 25 mag arcsec$^{-2}$, are taken from the PANBG. The PANBG is the largest homogeneous surface photometry data base of northern bright galaxies at present. The sample is a subset of the RSA galaxies. All the galaxies were observed with the 105 cm Schmidt telescope at Kiso Observatory (Takase et al. 1977) in the photographic $V$ band (Kodak IIa-D emulsion behind Schott GG 495 filter) during 1979–1988. Data reduction was carried out during 1988–1989 using the same data reduction system (Ichikawa et al. 1987) in order to keep the homogeneity of data. The internal accuracy is estimated to be 0.1 mag for the total magnitude and 0.04 in the axial ratio (PANBG).

The H I line widths $V_{HI}$ are taken from the catalog compiled by Huchtmeier & Richter (hereafter HR89, 1989). We use the line width at 20% of the peak intensity. When more than one measurement is given for a galaxy, the average value is used. HR89 gives a simple collection of many measurements obtained with various telescopes and data reduction systems, which can be identified in the references. We find that the systematic offsets are less than 10 km s$^{-1}$ among seven major references in HR89. After we finished all the computations for this work, Third Reference Catalogue of Bright Galaxies (de Vaucouleurs et al. 1991, hereafter RC3) was published. We checked the consistency of the line widths between our values adopted from HR89 and those given in RC3. Figure 1*a* shows the comparison of log $V_{HI}$ for 301 galaxies in the K90. A small systematic offset ($\sim 0.01$) is seen, but the correlation is sufficiently tight except for several labeled galaxies. A detailed examination of the HR89 references reveals that our values adopted from HR89 are more reliable for three of them (NGC 2715, NGC 2782, and NGC 3729). It is not clear, however, which value is better for the rest of them, which have only two independent measurements. We compare in Figure 1*b* the TF distances based on RC3 line widths with those based on our adopted values. No systematic offset is found here, although the same labeled galaxies show large discrepancies. Accordingly, we consider that our line widths adopted from HR89 form a sound data set for the purpose of this work, i.e., a data set at least no worse than that based on RC3 line widths.

In order to reduce the uncertainty of the inclination correction for line widths, we exclude galaxies with inclinations $i$ less than 45°. Most of the galaxies in the PANBG are found in HR89. Therefore, the PANBG determines the sample size of the K90.

### 2.2. *Calibration of the V Band TF Relation*

We calibrate the $V$ band TF (hereafter vTF) relation using nearby spiral galaxies whose distances have aleady been measured by independent methods, for instance, using Cepheid variables. The distance data for eight galaxies in the PANBG are given in Tammann (1987), which is a recent compilation of distances of nearby galaxies. We calibrate the vTF relation using the eight galaxies. The Galactic absorptions ($A_V^b$) are taken from Burstein & Heiles (1984). The internal absorption correction for total magnitudes ($A_V^i$) and inclination correction for line widths are computed by the methods given in Tully &

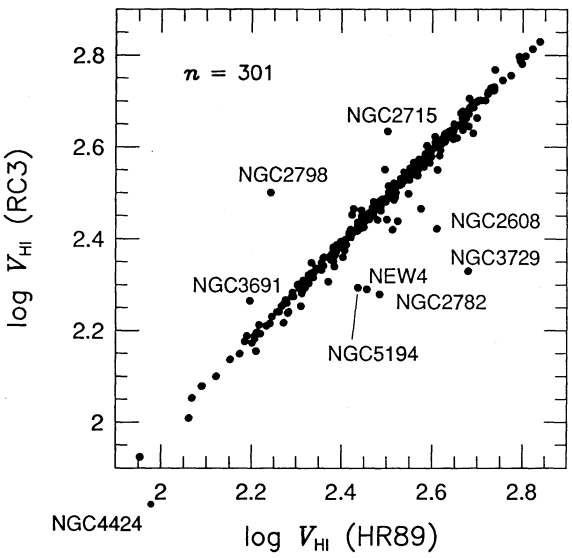


FIG. 1a

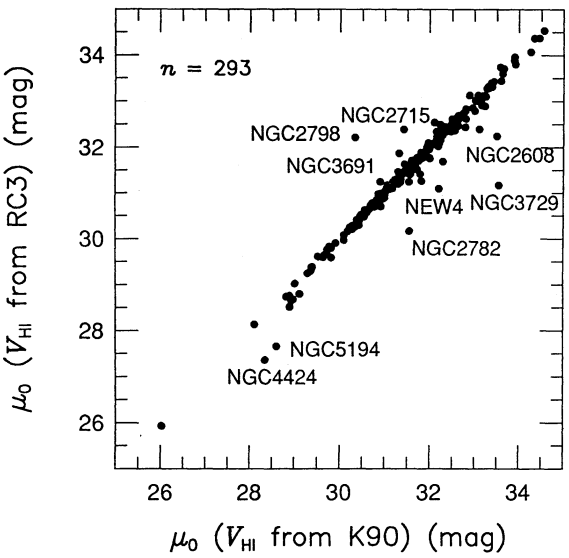


FIG. 1b

FIG. 1.—(*a*) Comparison of log $V_{H\,I}$ given in RC3 with those adopted from HR89. A total of 301 galaxies are plotted. Largely deviated galaxies are labeled. (*b*) Comparison of distance moduli based on $V_{H\,I}$ in RC3 and that in HR89. The local calibrators are rejected. In order to estimate the Malmquist bias, we set $\sigma_M = 0.3$ mag for the vTF relation derived from $V_{H\,I}$ in RC3.

Fouqué (1985). Thus, we calculate an absolute magnitude $M_V^{b,i}$ ($=m_V - A_V^b - A_V^i - \mu_0$, where $m_V$ and $\mu_0$ are an apparent total magnitude and a distance modulus, respectively) and a corrected line width $V_{H\,I}^c$ for each calibrator. The data for the calibrators are given in Table 1. Calibration is carried out by the weighted least-squares method with magnitudes and line widths being dependent and independent variables, respectively. The weight of each calibrator, which corresponds to the uncertainty of its distance, is taken from Fukugita et al. (1991). The vTF relation we obtain is

$$M_V^{b,i} = (-6.21 \pm 0.35) \log V_{H\,I}^c - (4.90 \pm 0.09) . \quad (1)$$

This vTF relation is shown in Figure 2. The vertical lines in Figure 2 are distance errors of the calibrators. The magnitude scatter in the vTF relation, $\sigma_M$, is only 0.3 mag. This value is as small as those in *R*, *I*, and *H* band TF relations given in Pierce & Tully (1988). We also define the vTF relation based on the four galaxies (NGC 224, NGC 598, NGC 2403, and NGC 3031) to which Freedman (1990) gives new distances using Cepheid variables. We find that the derived vTF relation is very similar to equation (1) with the slope of $-6.06 \pm 1.61$, the zero point of $-5.24 \pm 0.29$, and $\sigma_M$ of 0.6 mag, although the statistics is insufficient. We also find that these two vTFs give almost the same distance moduli to each galaxy in the K90 sample (the rms error and the offset are both only 0.03 mag). Accordingly, we use equation (1) for simplicity.

There are other slightly different estimates of Galactic absorption and different prescriptions for internal absorption correction (de Vaucouleurs, de Vaucouleurs, & Corwin 1976, hereafter RC2; RSA; Kodaira & Watanabe 1989). The calibrations of vTF based on these different methods are summarized in Appendix A. We find that the use of different calibrations does not affect the present analysis significantly since effects of the different methods cancel out on the average between the calibrators and the objective galaxies if the methods are applied consistently.

TABLE 1

BASIC DATA OF THE LOCAL CALIBRATORS

| Name (1) | Type (2) | $\mu_0$ (mag) (3) | $m_V$ (mag) (4) | $M_V^{b,i}$ (mag) (5) | log $V_{H\,I}^c$ (6) | $i$ (7) | Weight$^{-1}$ (8) |
|---|---|---|---|---|---|---|---|
| NGC 224..... | Sb | 24.2 | 3.28 | −21.75 | 2.71 | 75° | 0.20 |
| NGC 253..... | Sc | 27.5 | 7.17 | −20.82 | 2.63 | 70 | 1.00 |
| NGC 598..... | Scd | 24.4 | 5.56 | −19.33 | 2.29 | 58 | 0.30 |
| NGC 2366..... | Im | 27.8 | 11.23 | −17.18 | 1.99 | 69 | 0.82 |
| NGC 2403..... | Scd | 27.8 | 8.64 | −19.62 | 2.42 | 56 | 0.82 |
| NGC 3031..... | Sab | 28.7 | 7.12 | −22.05 | 2.69 | 59 | 1.10 |
| NGC 5204..... | Sm | 29.2 | 11.36 | −18.17 | 2.12 | 53 | 1.74 |
| NGC 5585..... | Sd | 29.2 | 10.98 | −18.53 | 2.23 | 52 | 1.74 |

NOTES.—Col. (2): Morphological type taken from the PANBG. Col. (3): Distance modulus taken from Tammann 1987. Col. (4): *V* band apparent magnitude taken from the PANBG. Col. (5): Total absolute magnitude corrected for Galactic and internal absorptions. Col. (6): Logarithm of corrected line width. Col. (7): Inclination. Col. (8): Inverse weight.

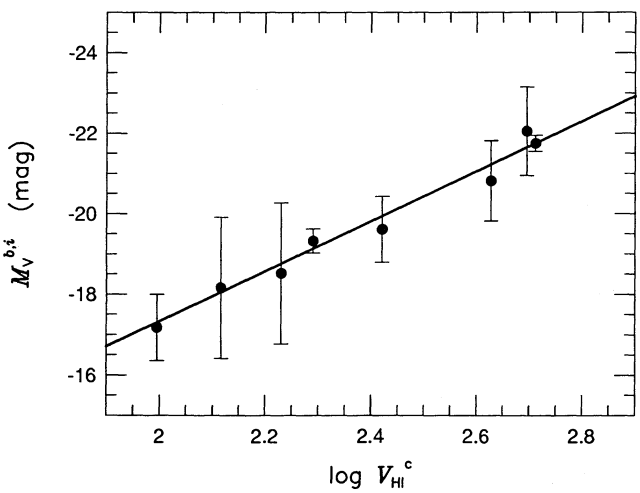


FIG. 2.—Local calibrators of the vTF relation. The vertical lines are distance errors of the calibrators (see text).

Using the vTF relation of equation (1), we estimate distances of galaxies other than the calibrators. Because the vTF relation has a finite scatter, we have to correct for the Malmquist bias effects (Malmquist 1920). Those galaxies which we deal with are mainly field galaxies, so we assume that their spatial distribution is uniform. In this case, the correction for the Malmquist bias is the same amount for every galaxy. The corrected distance modulus of a galaxy, $\mu_0$, is

$$\mu_0 = \mu_{\rm TF} + 1.38\sigma_M^2 , \quad (2)$$

where $\mu_{\rm TF} = m_V^{b,i} - M_V^{b,i}$ is the distance modulus calculated by equation (1) and $\sigma_M = 0.3$ mag, which is determined from the local calibrators, is the magnitude scatter of the vTF relation.

### 2.3. *Calculation of Peculiar Velocities*

When we compute the peculiar velocity $V_{\rm pec}$ of a galaxy at a distance $R$ and with an observed line-of-sight velocity $V_{\rm obs}$ (corrected to the CMB rest frame), it is convenient to use the expression

$$V_{\rm pec} = V_{\rm obs} - V_{\rm H}^0 \frac{R}{R_0} , \quad (3)$$

where $R_0$ is the distance of a galaxy or a cluster whose Hubble expansion velocity ($V_{\rm H}^0$) is known. The absolute value of $R$ is not necessary in this expression, and only the ratio $R/R_0$ is required. We are free from the problem of absolute scaling, i.e., the uncertainty of the Hubble constant, in the analysis of the velocity field by using this formalism.

In this study we use the Virgo Cluster as the reference cluster with the known $V_{\rm H}^0$. There are 15 galaxies in the PANBG which belong to the Virgo Cluster. Using these, we estimate the distance to the Virgo Cluster and calculate a distance ratio $R/R_0$ for each galaxy in the K90. The process of estimating the Virgo distance is presented in Appendix B.

### 2.4. *Comparison with the A82G and the 7S*

We compare the characteristics of the K90 with those of the two representative peculiar-velocity samples, the A82G and the 7S. A comment on the A82G may be relevant here. There are in total 308 galaxies in Aaronson et al. (1982)'s data set of peculiar velocity. Their distances were calculated from the TF relation in the $H$ band. They made aperture photometry in the $H$ band (Aaronson, Huchra, & Mould 1979, 1980), and accordingly axial ratios could not be estimated from their own observation. Therefore, they took the axial ratios from other catalogs such as RC2 or UGC (Nilson 1973). It is known that the mean distance error as measured by the scatter of the TF relation of 194 galaxies which have both diameters and magnitudes given in RC2 (this subsample is named A82G) is significantly smaller than that of the other galaxies (FB). In this paper we follow FB to use only the A82G in the analysis of the peculiar velocity field.

We estimate the rms distance error of the K90 galaxies as follows. For the 112 galaxies common to the K90 and the A82G (after rejecting the eight local calibrators), we examine the correlation between the distance moduli derived from the K90 and those given in the A82G and find the scatter to be 0.4 mag (see Fig. 3). The rms error of the distance moduli of the A82G galaxies is estimated to be about 0.3 mag by FB and Han & Mould (1990). Accordingly, the error of the K90 galaxies is estimated to be $(0.4^2 - 0.3^2)^{1/2} \sim 0.3$ mag. This value is as good as that of the A82G and it is also consistent with the scatter of our local calibrators. The offset of $\sim 0.4$ mag seen in Figure 3 is due to the different choice of calibrator distances between the K90 and the A82G. As will be seen in Figure 5, the sampling depth of the K90 is deeper than that of the A82G. Accordingly, the K90 contains more galaxies than the A82G. In summary, the K90 is almost the same in the distance accuracy but 1.5 times as large in the sample size as the A82G.

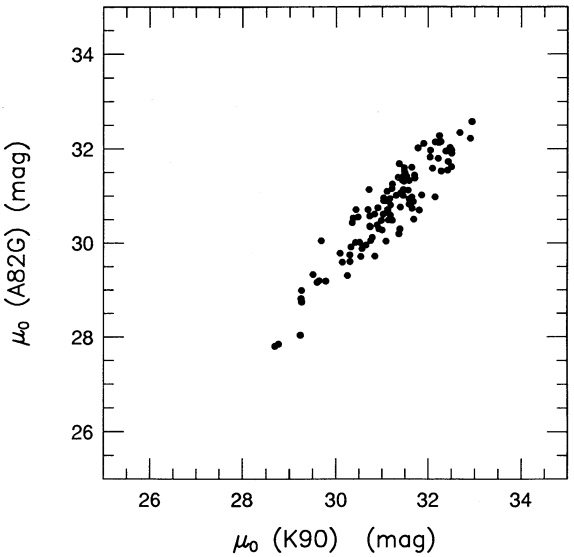


FIG. 3.—Comparison of distance moduli for galaxies common to the K90 and the A82G. The rms scatter is 0.4 mag. The offset of 0.41 mag is due to the difference in the zero point of the absolute calibration between the $V$ band and the $H$ band TF relations. This value is roughly consistent with the difference of the distance modulus of Virgo between the K90 and the A82G (31.33 and 30.82 mag, respectively).

We compare the K90 with the 7S next. The 7S is a deep-sampled data set which reaches as far as $V_{\rm H} \sim 8000$ km s$^{-1}$, and its sky coverage is wide. In particular, it includes many galaxies located near the postulated GA. In these points the 7S is a better sample than the K90 and the A82G in the study of the large-scale velocity field around the LS. On the other hand, distances of the 7S galaxies are determined by the $D_n$-$\sigma$ relation (Dressler et al. 1987b) and the error in the distance modulus is 0.4–0.5 mag (FB), which is larger than those of the K90 and the A82G. The number density of the 7S galaxies is low in the LS, in particular, in our neighborhood where the LA may exist. Therefore, the K90 is more suitable than the 7S for examining the velocity field within the LS and the existence of the LA. The sky distributions of galaxies of these three samples are shown in Figure 4.

## 3. QUALITATIVE OVERVIEW OF THE VELOCITY FIELD

Figure 5 shows the positions and the peculiar velocities with respect to the CMB of the K90 galaxies projected on the supergalactic $X$-$Y$ plane (SG plane). Coordinates are in units of $H_0 R$, namely km s$^{-1}$, and the LG is at $(X, Y) = (0, 0)$. The length of the bar of each galaxy corresponds to the amplitude of its peculiar velocity. Galaxies with outward bars from us have positive peculiar velocities and those with inward bars have negative velocities. It is seen in Figure 5 that galaxies in some regions have systematic peculiar velocities. Most of the galaxies in a sector along $Y = -X$ in the second quadrant ($X < 0$, $Y > 0$) have $V_{\rm pec} > 0$. They move away from us at velocities of several hundreds of km s$^{-1}$. Except for this region,

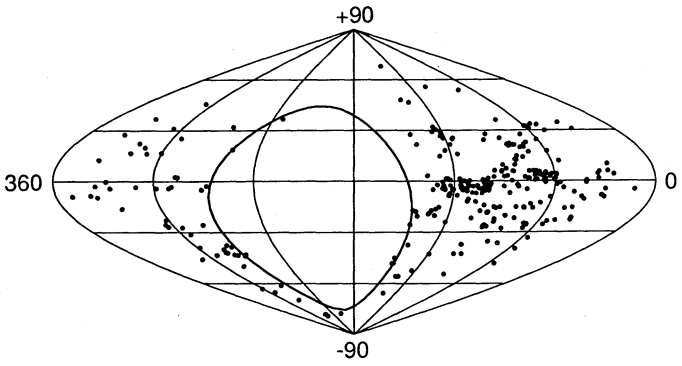


FIG. 4a

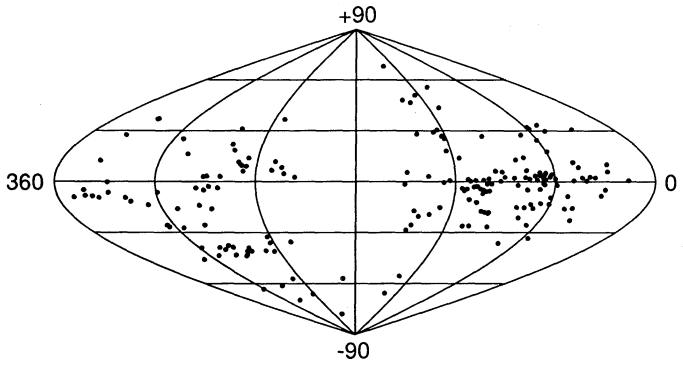


FIG. 4b

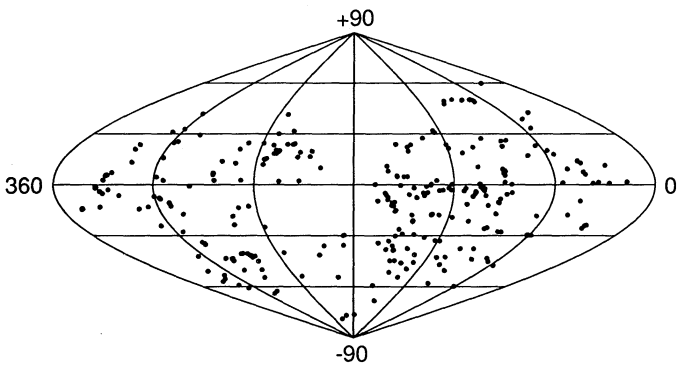


FIG. 4c

FIG. 4.—The distributions of galaxies in (*a*) the K90, (*b*) the A82G, and (*c*) the 7S. $L$ and $B$ are supergalactic longitude and latitude, respectively. The solid line in (*a*) is $\delta = -30°$, which roughly corresponds to the practical limit of observation at Kiso Observatory. The prominent structures at $(L, B) \sim (100°, 0°)$ and $(L, B) \sim (60°, 0°)$ are the Virgo Cluster and Ursa Major cluster, respectively.

there are few regions where galaxies have systematically positive peculiar velocities. A region of negative velocity is seen at $(X, Y) \sim (500, 1000)$, where the Ursa Major cluster is located. Nearby galaxies in $0 \lesssim X \lesssim 1000$ and $-1000 \lesssim Y \lesssim 0$ also have $V_{\rm pec} < 0$. As is seen quantitatively in the next section, the direction of motions of these nearby galaxies is almost the same as that of the LG motion as a whole.

In order to see the global motions of galaxies more clearly, we make maps of the smoothed velocity field using the smoothing method given in Bertschinger et al. (1990). Namely, the radial velocity $u$ at position $\boldsymbol{r}$ (LG is at $\boldsymbol{r} = 0$) is computed as

$$u(\boldsymbol{r}) = \sum_i [\hat{\boldsymbol{r}} \cdot \boldsymbol{A}^{-1}(\boldsymbol{r}) \cdot \hat{\boldsymbol{r}}_i] W(r, r_i) V^i_{\rm pec} , \quad (4)$$

where

$$\boldsymbol{A} = \sum_i W(r, r_i) \hat{\boldsymbol{r}}_i \hat{\boldsymbol{r}}_i , \quad (5)$$

and

$$W(r, r_i) = \frac{R_4^3(r_i)}{\sigma_i^2} \exp\left[ -\frac{(\boldsymbol{r} - \boldsymbol{r}_i)^2}{2R_5^2} \right] . \quad (6)$$

Here $\boldsymbol{r}_i$ is the distance of the $i$th galaxy, $\hat{\boldsymbol{r}} = \boldsymbol{r}/r$ and $\hat{\boldsymbol{r}}_i = \boldsymbol{r}_i/r_i$ are the unit vectors, $\sigma_i^2 = \sigma_v^2 + (H_0 \boldsymbol{r}_i \cdot \Delta)^2$ is the inverse weight of the $i$th galaxy, $\sigma_v$ is the velocity dispersion of spirals, $\Delta$ is the distance error in linear scale, $R_4(r_i)$ is the distance from the $i$th galaxy to its fourth nearest neighbor, and $R_5$, the smoothing radius, is the distance from the position $\boldsymbol{r}$ to the fifth nearest neighbor. We assume $\sigma_v = 200$ km s$^{-1}$. Figure 6 shows the smoothed velocity field in the SG plane expressed in the form of the contour map. Each contour corresponds to the same $V_{\rm pec}$. Solid and dashed contours are $V_{\rm pec} > 0$ and $< 0$, respectively. The bold line shows the boundary within which the map is reliable. Outside of the boundary, the number density of sample galaxies is lower than $\sim 1$ galaxy per (1000 km s$^{-1}$)$^3$. The velocity field in the SG plane within the boundary looks like a dipole pattern with the negative side slightly weak.

We also construct three-dimensional peculiar-velocity vector maps in order to compare the present result with the similar maps by Bertschinger et al. (1990), which are mainly based on the A82G and the 7S. We follow the method given by them. In the comparison of the three-dimensional velocity maps emphasis should be put on the global structure since

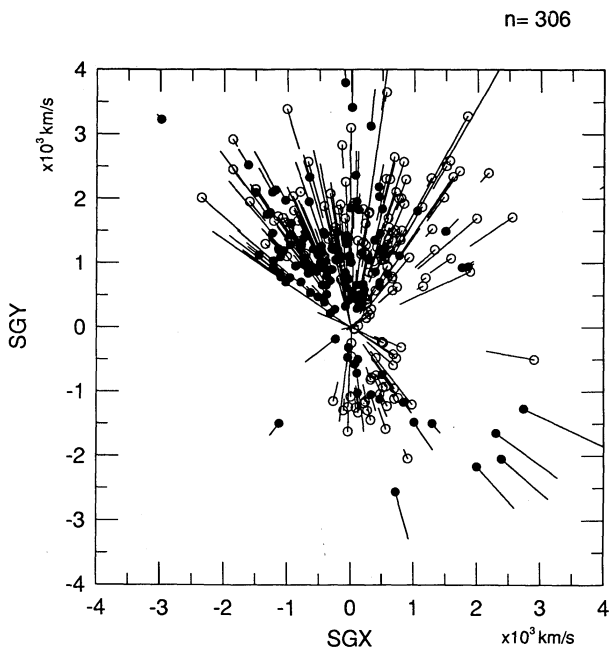


FIG. 5.—Peculiar velocities of the K90 galaxies. The galaxies are projected on the $X$-$Y$ plane (SG plane). Coordinates are in units of $H_0 R$, namely km s$^{-1}$. The length of the bar of each galaxy corresponds to the amplitude of the peculiar velocity. Galaxies with outward bars from us have positive peculiar velocities and those with inward bars have negative peculiar velocities.

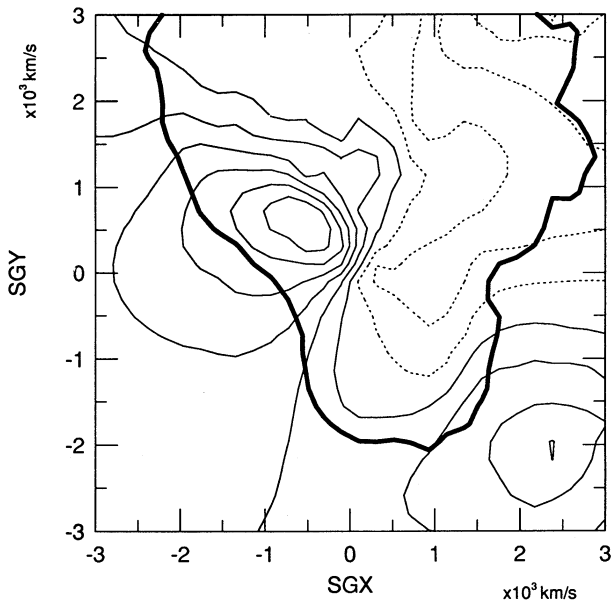


FIG. 6.—Smoothed peculiar velocity field on the SG plane based on the K90. The smoothing procedure is taken from Bertschinger et al. (1990). Each contour corresponds to the same $V_{pec}$. The interval of contours is 200 km s$^{-1}$. Solid and dashed contours are $V_{pec} > 0$ and $V_{pec} < 0$, respectively. The bold line shows the boundary within which the map is reliable. Outside of the boundary, the number density of sample galaxies is lower than $\sim 1$ galaxy per (1000 km s$^{-1}$)$^3$.

local details are easily affected by a slight change in smoothing procedures. Figure 7 shows the two components ($V^X_{pec}$, $V^Y_{pec}$) of three-dimensional peculiar velocities in the SG plane. Comparing Figure 7 with Figure 6*a* of Bertschinger et al. (1990), we find that the velocity fields shown in the two maps are basically similar to each other. In the $Y > 0$ region, the systematic motion is almost antiparallel to the $X$ axis. On the other hand, galaxies in $X > 0$ and $Y < 0$ move toward the second quadrant. The motion in the LS looks like, as a whole, an infall toward a position of $(X, Y) \sim (-3000, 1000)$, rather than a bulk motion. Another important point is that we cannot see the Virgo infall pattern very clearly either in Figure 7 or in Figure 6*a* of Bertschinger et al. (1990). This indicates that the Virgo Cluster, which is located at $(X, Y) \sim (0, 1300)$, has little gravitational influence on galaxies in the LS.

## 4. QUANTITATIVE ANALYSIS

We apply in this section the GA model to the K90 and determine the GA parameters. Our motivation to do this is twofold. First, according to the analysis by FB, the A82G and the 7S give different GA positions. The distance to the GA obtained from the A82G is shorter than that from the 7S although the directions of the GA agree. This suggests that the global motion of galaxies in the LS may differ from that of more distant galaxies or that the motions of spirals and ellipticals may be different. However, the sampling depth of the A82G is shallow, and on the other hand, the number density of the 7S galaxies in the LS is low. It is important to estimate independently the GA parameters using the K90 in order to examine the reliability of the GA parameters obtained from the A82G.

Second, FB found from the analysis of the A82G that our nearby galaxies (those with $V_H \lesssim 700$ km s$^{-1}$) move together to a direction different from that predicted by the GA model. They called this difference the Local Anomaly (LA) and interpreted it as due to a nearby density fluctuation. However, the source of the LA has not been identified yet. Before searching for the source, we reanalyze the nearby velocity field using the K90 and examine whether the global and the nearby motions differ or not.

We determine the GA parameters using the K90. The primary aim is to investigate the global motion in the LS using the GA model, rather than to determine the position of the GA itself. We regard here the GA model as a simple approximation to explain the velocity field in the LS.

The GA model we use includes the following parameters: (1) $V_A$, the GA infall velocity at the LG, (2) ($L_A$, $B_A$), the supergalactic coordinates of the GA, (3) $H_0 R_A$, the distance to the GA (km s$^{-1}$), and (4) $V_V$, the Virgo infall velocity at the LG.

Following Han & Mould (1990) we describe the GA infall velocity at a distance $x$ from the GA by

$$V_A(x) = V_A\left(\frac{x}{R_A}\right)^{-1}, \quad (7)$$

and the Virgo infall velocity at a distance $y$ from Virgo by

$$V_V(y) = V_V\left(\frac{y}{R_V}\right)^{-1}, \quad (8)$$

where $R_A$ and $R_V$ are the distances of the GA and Virgo from the LG, respectively.

FB introduced in their GA model the cores of the GA and Virgo so that infall velocities converge at the both centers, but here we do not assume the core either in the GA or in Virgo. The reason for this simplification is as follows. In the 7S, the core radius of the GA is determined by galaxies near the GA. However, there are few galaxies near the GA in the K90 as well as in the A82G, and, as is said by FB themselves, the distribution of galaxies in the GA region is clumpy. Consequently, it is not realistic to assume a spherically symmetric core. The form

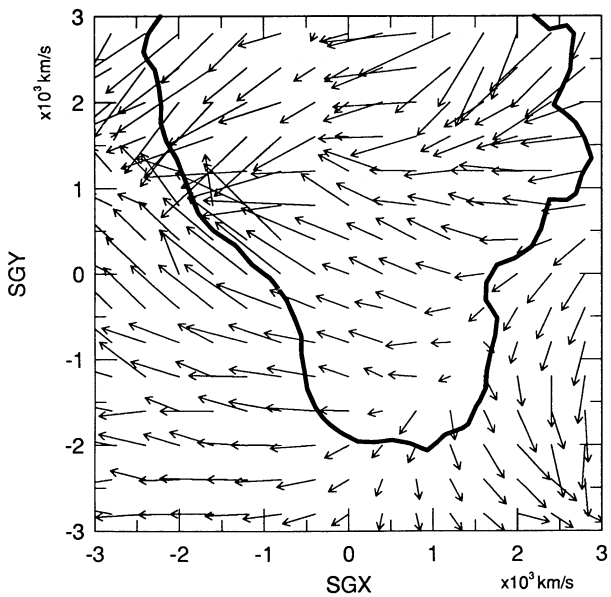


FIG. 7.—Three-dimensional velocity map on the SG plane based on the K90 constructed by the method given in Bertschinger et al. (1990). An arrow is the vector sum of $V^X_{pec}$ and $V^Y_{pec}$. The bold line is the same as in Fig. 6.

of the GA infall velocity given in FB is

$$V_A(x) = V_A\left(\frac{x}{R_A}\right)\left[\frac{1+c_A^2}{(x/R_A)^2+c_A^2}\right]^{1.35}, \quad (9)$$

where $c_A = 0.34$ is the dimensionless core radius. The difference between equations (7) and (9) has little influence on the GA parameters other than $c_A$ in the region where the K90 covers. We also exclude from the analysis the galaxies within 6° from the Virgo center (NGC 4486) on the sky. This region is generally regarded as the Virgo core. Therefore, we consider that the formulae (7) and (8) are adequate for the present analysis. We also exclude galaxies whose distances from the LG are smaller than 1000 km s$^{-1}$ in order to avoid the influence of the LA, if any, on the model parameters.

The model parameters presented above are determined by the maximum likelihood method. The most probable values of these parameters are those which give the likelihood function the maximum value. The likelihood function $L$ is expressed as

$$L = \sum_i \ln \frac{1}{\sqrt{2\pi}\,\sigma_i} \exp\left[-\frac{(V^i_{\rm pre} - V^i_{\rm obs})^2}{2\sigma_i^2}\right], \quad (10)$$

where,

$$\sigma_i^2 = \sigma_v^2 + (H_0 r_i \cdot \Delta)^2 . \quad (11)$$

Here $V^i_{\rm pre}$ is the predicted velocity of the $i$th galaxy, $r_i$ is its distance, $\sigma_v$ is the velocity dispersion of field spiral galaxies, and $\Delta$ is the distance error in linear scale. Different values of $\sigma_v$ in the range of 100–200 km s$^{-1}$ are found to have little influence on the GA parameters. The model fitting is made to the A82G as well as to the K90 to allow for a straight comparison of the two samples. GA parameters obtained for the K90 and the A82G are tabulated in Table 2. The GA parameters for the 7S determined by FB are also presented in Table 2. We find that the parameters for the K90 are roughly consistent with those for the 7S and the A82G. The directions of the GA differ by about 30° in the three samples, but this inconsistency is not so large in a naive sense. The Virgo infall velocity is small in all the three samples, so the Virgo infall is not a major source of the velocity field in the LS. Aaronson et al. (1982a) obtained ~250 km s$^{-1}$ for the Virgo infall velocity at the LG. This value is significantly larger than $V_V$ we obtain here. FB have already investigated the reason why Aaronson et al. derived the large value. FB claimed that, since Aaronson et al. assumed the Virgo infall only, they misinterpreted "the tidal compression" along the *SGY* axis due to the GA infall as the Virgo infall. We essentially agree with their claim. As seen in Figure 7, the peculiar motion in the LS is similar to an infall motion towards a single source outside the LS (see also Figs. 6 and 14 of Bertschinger et al. 1990). Therefore, the claim by FB is valid irrespective of the existence of the GA.

Thus, if we try to explain the observed velocity field in the LS in the framework of a model with two infall sources, we obtain almost the same solution, whichever sample of the K90, the A82G, and the 7S is used. The solution is that there is a dominant infall source which causes a large-scale ($V_H \sim 4000$ km s$^{-1}$) and large-amplitude ($V_{\rm pec} \sim 500$ km s$^{-1}$ at the LG) infall motion roughly in the direction of the Hydra-Centaurus supercluster. This is expected from the qualitative overview of the velocity field described in § 4. The observed velocity field in the LS looks like a infall motion toward a single source.

The difference of about 30° in the direction of the GA among the three samples is, however, significant in terms of the existence of the LA. As we demonstrate below, all galaxies within several hundred km s$^{-1}$ from the LG move in concert with the LG. This is also shown by several other studies (e.g., Peebles 1988, FB, Han & Mould 1990). According to Lubin & Villela (1986), the solar motion relative to the CMB is 360 km s$^{-1}$ toward $(l, b) = (265°, 50°)$. Therefore, the LG motion with respect to the CMB is 600 km s$^{-1}$ toward $(L, B) = (138°, -38°)$ after correcting the "standard" solar motion with respect to the LG centroid, i.e., $V_\odot = 300$ km s$^{-1}$ toward $(l, b) = (90°, 0°)$ (de Vaucouleurs et al. 1976).

First, we examine the reality of this systematic motion of the nearby galaxies. We divide galaxies of the K90 in groups by a distance interval of 250 km s$^{-1}$ and estimate the bulk motion velocity and its apex for each group. The same analysis is carried out for the A82G for comparison. The bulk motion solutions are set out in Table 3 for both samples. Groups with distances smaller than 250 km s$^{-1}$ are excluded because the numbers of galaxies are too small. For both samples the bulk motion solutions of groups nearer than 750 km s$^{-1}$ agree with the LG motion with respect to the CMB within errors. Therefore it is concluded that galaxies within about 750 km s$^{-1}$ move to almost the same direction and at almost the same velocity as the LG. At distances larger than 1000 km s$^{-1}$, bulk motion solutions do not agree with the LG motion. The Virgo Cluster exists in the range of $1000 < V_H < 1500$ km s$^{-1}$, and the random velocities of galaxies in and around Virgo are often large. This may be the reason for the disagreement with the LG motion.

Second, we compare the observed motion of the LG, which is almost the same as the systematic motion of the nearby galaxies with $V_H \lesssim 700$ km s$^{-1}$, with its motion predicted by the GA model. If these two values agree, it will be concluded

TABLE 2

GA PARAMETERS DETERMINED FROM THE THREE SAMPLES

| Sample (1) | $L_A$[a] (2) | $B_A$[a] (3) | $H_0 R_A$[b] (km s$^{-1}$) (4) | $V_A$[c] (km s$^{-1}$) (5) | $V_V$[d] (km s$^{-1}$) (6) | $\Delta\theta$[e] (7) |
|---|---|---|---|---|---|---|
| K90 ..... | 150° ± 4° | −30° ± 5° | 3708 ± 297 | 456 ± 51 | 38 ± 26 | 13° |
| A82G ..... | 159 ± 9 | −6 ± 4 | 2684 ± 497 | 444 ± 87 | 86 ± 37 | 37 |
| 7S[f] ..... | 161 ± 10 | −6 ± 10 | 4200 ± 350 | 535 ± 70 | ~100 | 38 |

[a] Supergalactic longitude and latitude of the GA.
[b] Distance to the GA.
[c] GA infall velocity at the LG.
[d] Virgo infall velocity at the LG.
[e] Difference between the GA direction and the CMB apex of the LG.
[f] Parameters are those determined by FB.

TABLE 3

BULK MOTION SOLUTIONS OF NEARBY GALAXIES

| Distance Range (km s$^{-1}$) (1) | $L_B$[a] (2) | $B_B$[a] (3) | $V_B$[b] (km s$^{-1}$) (4) | $n$[c] (5) |
|---|---|---|---|---|
| A. K90 | | | | |
| 250–500 | 142° ± 6° | −31° ± 20° | 865 ± 240 | 13 |
| 500–750 | 146 ± 9 | −27 ± 15 | 720 ± 103 | 16 |
| 750–1000 | 154 ± 7 | −21 ± 8 | 740 ± 110 | 26 |
| 1000–1250 | 158 ± 7 | −7 ± 14 | 615 ± 95 | 39 |
| 1250–1500 | 166 ± 7 | −49 ± 9 | 835 ± 119 | 34 |
| B. A82G | | | | |
| 250–500 | 146° ± 8° | −31° ± 38° | 715 ± 352 | 10 |
| 500–750 | 144 ± 10 | −29 ± 23 | 510 ± 116 | 15 |
| 750–1000 | 156 ± 9 | −21 ± 11 | 530 ± 100 | 24 |
| 1000–1250 | 166 ± 7 | −19 ± 16 | 705 ± 149 | 18 |
| 1250–1500 | 174 ± 6 | −7 ± 14 | 565 ± 142 | 31 |

[a] Supergalactic longitude and latitude of the apex of the bulk motion.
[b] Amplitude of the bulk motion.
[c] Number of galaxies.

that the motion of the LG and its nearby galaxies is similar to the global motion of galaxies in the LS. We compare in Table 4 the observed motion of the LG with the predicted motion by three GA models based on the three samples. We find that the LG motions predicted by the A82G and the 7S, in particular, the components along the $Z$ axis, are significantly different from the observed values. The major reason for this is that the GA directions by the A82G and the 7S differ from the direction of the LG motion by 37° and 38°, respectively. Because FB believed that the direction of their GA is correct, they had to introduce a gravitational perturbation to explain this discrepancy of the LG motion. However, the GA direction predicted by the K90 is fairly close to that of the observed motion ($\Delta\theta = 13°$). Therefore, on the basis of the K90, the observed LG motion may be explained with only one infall source (and a very weak Virgo infall) without invoking other local density perturbation, although the difference of 13° is outside of the nominal error bars.

Then, one has a question: Why the GA parameters, in particular, the direction of the GA, differ among the three samples? This may be due to the difference of sampled regions (if so, the GA model may be regarded as an oversimplified model with the present status of available data), or to the difference in the method of distance determination. To answer the question, we make four subsamples from the K90, the A82G, the 7S, and RSA, and then estimate the GA parameters

TABLE 4

DIFFERENCE BETWEEN THE PREDICTED AND OBSERVED LG MOTIONS

| Sample (1) | $\Delta V^X$ (km s$^{-1}$) (2) | $\Delta V^Y$ (km s$^{-1}$) (3) | $\Delta V^Z$ (km s$^{-1}$) (4) | $\Delta\theta$ (5) |
|---|---|---|---|---|
| K90 | 2 ± 75 | 81 ± 85 | −143 ± 63 | 13° |
| A82G | 83 ± 126 | 73 ± 143 | −323 ± 46 | 37 |
| 7S | 177 ± 95 | 45 ± 119 | −313 ± 111 | 38 |

NOTES.—Superscripts $X$, $Y$, and $Z$ imply the $X$, $Y$, and $Z$ axis components, respectively. Col. (2): $\Delta V^X = V^X_{CMB} - V^X_A - V^X_V$. Col. (3): $\Delta V^Y = V^Y_{CMB} - V^Y_A - V^Y_V$. Col. (4): $\Delta V^Z = V^Z_{CMB} - V^Z_A - V^Z_V$. Here $V_{CMB}$ is the observed peculiar velocity of the LG with respect to the CMB. Col. (5): Difference between the GA direction and the CMB apex of the LG.

using them to compare the results. The subsamples we make are as follows:

(S1).—Galaxies common to the K90 and the A82G. The data are taken from the K90 (namely, distances are by the $V$ band TF relation).

(S2).—The same galaxies as the S1, but the data are from the A82G (i.e., distances are by the $H$ band TF relation). We assume the scatter of the $H$ band TF relation to be 0.3 mag.

(S3).—The 7S galaxies located in the range of 1000 km s$^{-1}$ $< H_0 R <$ 2500 km s$^{-1}$. This range roughly corresponds to that of the K90. The data are taken from the 7S, i.e., distances are by the $D_n$-$\sigma$ relation.

(S4).—The same galaxies as the K90, but apparent magnitudes are taken from RSA, and distances are determined by the $B$ band TF relation. We calibrate the $B$ band TF relation by the same galaxies as in the K90 and set the scatter of the $B$ band TF relation to be 0.4 mag.

The pair of the S1 and S2, and that of the S4 and K90 are used to examine the influence of the different methods of distance determination, namely the $V$ band, the $H$ band, and the $B$ band TF relations. We cannot extend this comparison to the $D_n$-$\sigma$ relation because the TF relation is the spirals and, on the other hand, the $D_n$-$\sigma$ is for ellipticals. If it is found that the difference of photometric bands in the TF relation does not influence the GA solutions, then differences of sampling regions will be a major source of the discrepancy.

The GA parameters obtained from the subsamples above are summarized in Table 5. The GA distances derived from the S1 and the S2 have large uncertainties because the depth of these samples is very shallow (see Fig. 3). However, the other parameters based on the S1 and the S2 have small errors and agree with each other within errors. This is also the case between the parameters based on the S4 and the K90. Therefore, the difference of photometric bands of the TF relation has little influence on the GA parameters. The reason for the discrepancy of the GA direction among the K90 and the A82G is, thus, likely to be the difference of sample galaxies.

Based on this assumption, we try to find specific regions in the LS which cause the discrepancy of the GA direction among the samples. However, we find that such a specific region does not exist. It is, of course, true that the number density of sample galaxies is low and the peculiar-velocity data are noisy, but we think that the GA model is too simple to delineate the local peculiar velocity field and to discuss the existence of the LA. However, we suppose that the new result from the K90 is convincing that the global motion in the LS agrees with the LG motion because the K90 is superior to the A82G in terms of the number of galaxies available to the model fitting and the sampling depth. This is supported by the fact that the S3, which has roughly a similar sampling depth to that of the K90, gives the GA direction closer to that based on the K90 than that based on the A82G. According to the new result, the motion of the LG represents well that of the LS. Recently, Scaramella, Vettolani, & Zamorani (1991) examined the distribution of clusters of galaxies in Abell (1958) and ACO (Abell, Corwin, & Olowin 1989) catalogs. They concluded that the optical dipole, which corresponds to the acceleration of gravity, of clusters within ~300 Mpc is very close to the direction of the LG motion with respect to the CMB (CMB apex). If this is true, the direction of the LG motion is a very specific direction not only in the LS but also in such a large region. This direction is, however, different from the GA direction

TABLE 5

GA PARAMETERS DETERMINED FROM THE FOUR SUBSAMPLES

| Sample (1) | $L_A$[a] (2) | $B_A$[a] (3) | $H_0 R_A$[b] (km s$^{-1}$) (4) | $V_A$[c] (km s$^{-1}$) (5) | $V_V$[d] (km s$^{-1}$) (6) | $\Delta\theta$[e] (7) | $n$ (8) |
|---|---|---|---|---|---|---|---|
| S1..... | 164° ± 8° | −28° ± 9° | 9270 ± 6180 | 566 ± 84 | 107 ± 45 | 24° | 80 |
| S2..... | 171 ± 8 | −21 ± 11 | 4831 ± 2577 | 521 ± 94 | 87 ± 46 | 33 | 78 |
| S3..... | 159 ± 4 | −22 ± 2 | 2666 ± 240 | 382 ± 79 | −40 ± 97 | 24 | 54 |
| S4..... | 154 ± 8 | −29 ± 9 | 4079 ± 853 | 497 ± 65 | 8 ± 54 | 16 | 226 |

[a] Supergalactic longitude and latitude of the GA, respectively.
[b] Distance to the GA.
[c] GA infall velocity at the LG.
[d] Virgo infall velocity at the LG.
[e] Difference between the GA direction and the CMB apex of the LG.

obtained by FB. New peculiar-velocity surveys of a larger depth are needed in order to examine the large-scale motion beyond the LS in more detail.

## 5. SUMMARY AND CONCLUSIONS

We study the velocity field in the Local Supercluster on the basis of a newly compiled sample of 306 spiral galaxies (K90 sample) as well as two previous samples, i.e., the A82G and the 7S. The K90 is the largest sample of spiral galaxies available at present with distance estimates as good as those for the A82G ($\sigma_M = 0.3$ mag in the distance modulus). Galaxy distances in the K90 are determined in this study using the Tully-Fisher relation while those in the A82G and the 7S are taken from the original literature. The elliptical and spiral samples are complementary. The elliptical sample (7S) covers a larger volume of space but with a lower resolution than the spiral samples (A82G and K90).

First, we find in the LS a coherent motion toward a direction close to the CMB apex of the LG ($\Delta\theta = 13°$–$38°$) in the K90 as well as in the A82G and 7S. Second, we apply a slightly simplified version of the standard GA model to the K90 and the A82G and determine the model parameters by the identical procedures. These parameters are compared with those obtained by FB from the 7S. We find a broad agreement in the model parameters. However, the direction of the GA is different by at most 26° among the three samples. The difference is significant in terms of the Local Anomaly. The direction of the GA obtained from the K90 is different from the CMB apex of the LG by only 13° while the difference amounts to 37° and 38° for the A82G and the 7S, respectively. This indicates that it is not necessary to invoke the Local Anomaly in the K90 unlike the other two samples.

It is found that the galaxies common to the K90 and the A82G give almost the same direction of the GA ($\Delta\theta = 9°$) for two different sets of distances. It is also found that when we impose on the 7S a shallower depth similar to the depth of the K90, the GA direction from the 7S approaches the direction determined from the K90. The disagreement in the direction of the GA among the three samples is thus mainly due to the difference of sampling regions. This may imply that the GA model, which is a model to describe the global motion in the LS, is too simple to discuss the significance of the Local Anomaly. Much larger samples with higher resolution are necessary to delineate the detailed local peculiar velocity field.

We would like to thank K. Kodaira, M. Umemura, and S. Ichikawa for critical reading of the manuscript, M. Fukugita and M. Doi for many valuable discussions, and N. Yasuda for information on the statistical properties of the H I data. We also thank the referee, J. P. Huchra, for constructive comments which improved the present paper.

## APPENDIX A

## CALIBRATION OF THE vTF RELATION BASED ON DIFFERENT CORRECTION METHODS FOR GALACTIC AND INTERNAL ABSORPTIONS

When we calibrate the vTF relation in § 2, Galactic absorptions are taken from Burstein & Heiles (1984, hereafter BH) and internal absorption is computed by the method given in Tully & Fouqué (1985, hereafter TF85). There are, however, other estimates for Galactic absorptions and different prescriptions for internal absorption correction. We present here the vTF relations calibrated by other combinations of the methods. It is found that the results of the present study do not change significantly whichever calibration is adopted if the correction methods are consistently applied to the calibrators and to the object galaxy. The correction methods we take are the followings.

Galactic absorption is taken from (*a*) BH, (*b*) RC2, and (*c*) RSA. Estimates given in (*a*) are based on the observation of H I column density. The prescription given in (*b*) is well approximated by

$$A_V^b = 0.15 \csc |b| ,$$

and that given in (*c*) by

$$A_V^b = 0.10 (\csc |b| - 1) \qquad (|b| < 50°)$$
$$= 0 \qquad (|b| > 50°) ,$$

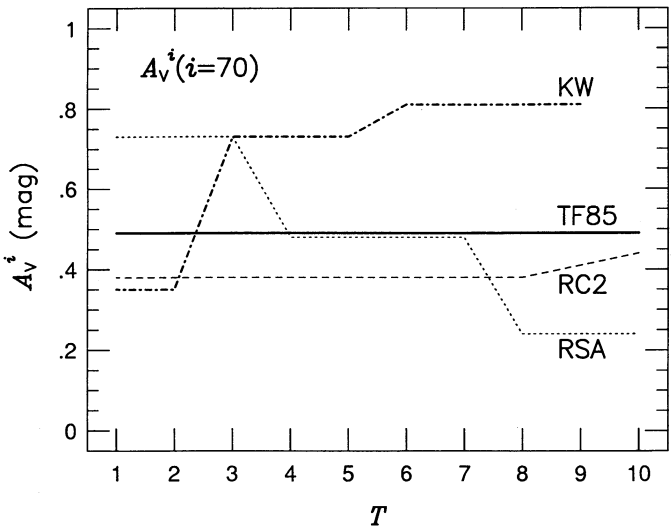


FIG. 8.—The amount of total, internal absorption at $i = 70°$ estimated by the four prescriptions as a functions of the morphological type index $T$. We add 0.13 mag to RC2's estimates to obtain total absorptions (see text).

where $b$ is Galactic latitude. As $|b|$ is larger, the amount of absorption estimated by (*a*) and (*c*) vanishes while that by (*b*) has a finite value ($A_V^b \approx 0.15$ mag). The difference of $A_V^b$ between (*b*) and (*c*) is roughly 0.2 mag in the range of $|b| > 30°$.

Methods of the internal absorption correction $A_V^i$ are taken from (*a*) TF85, (*b*) RC2, (*c*) RSA, and (*d*) Kodaira & Watanabe (1988, hereafter KW). The prescriptions in (*a*) and (*b*) give nearly constant amount of correction among all the morphological types (Sa–Im). The amount of correction given in (*c*) decreases while that given in (*d*) increases when the morphological type becomes later. As an example, we show in Figure 8 the amount of correction at $i = 70°$ estimated by these four prescriptions as a function of $T$, where $T$ is the morphological type index in RC2. Here, $A_V^i$ based on the RC2 method is the differential absorption relative to the face-on absorption ($A_V^{i=0}$) while that computed by the other three methods is the *total* absorption. Therefore, we add the face-on absorption, $0.17 \times \frac{3}{4} = 0.13$ mag, to a RC2 estimate in order to obtain a total absorption (see RC2).

The vTF relations for the eight calibrators based on the 12 ($3 \times 4$) combinations of Galactic and internal absorption corrections are given in Table 6.

We find that whichever combinations we use the magnitude scatter is as small as $\sigma_M \sim 0.3$ mag. It is shown in Appendix B that the difference of absorption correction methods has little influence on the determination of the Virgo distance.

## APPENDIX B

## DISTANCE TO THE VIRGO CLUSTER ESTIMATED BY THE vTF RELATION

### B1. DISTANCE TO THE VIRGO S CLOUD

We estimate the Virgo distance using the K90 by the vTF relation. We regard a galaxy as a Virgo member when it has $\theta < 6°$ and $V_{obs} < 3000$ km s$^{-1}$, where $\theta$ is the angular separation from the Virgo center (NGC 4486) and $V_{obs}$ is the observed recession velocity. The region of $\theta < 6°$ is regarded as the core of the Virgo Cluster. There are 40 spiral galaxies in the K90 which satisfy this criterion.

TABLE 6

SLOPE AND ZERO POINT OF THE vTF RELATION DERIVED ON THE BASIS OF THE 12 COMBINATIONS OF DIFFERENT METHODS FOR GALACTIC AND INTERNAL ABSORPTIONS[a]

| | $A_V^i$ | | | |
|---|---|---|---|---|
| $A_V^b$ | TF85 | RC2 | RSA | KW |
| | A. Slope | | | |
| BH | $-6.21 \pm 0.35$ | $-6.05 \pm 0.36$ | $-6.77 \pm 0.42$ | $-6.01 \pm 0.41$ |
| RC2 | $-6.08 \pm 0.31$ | $-5.91 \pm 0.33$ | $-6.63 \pm 0.38$ | $-5.90 \pm 0.33$ |
| RSA | $-6.15 \pm 0.33$ | $-5.99 \pm 0.34$ | $-6.71 \pm 0.40$ | $-5.95 \pm 0.37$ |
| | B. Zero Point | | | |
| BH | $-4.90 \pm 0.09$ | $-5.07 \pm 0.09$ | $-3.62 \pm 0.11$ | $-5.64 \pm 0.09$ |
| RC2 | $-5.33 \pm 0.08$ | $-5.50 \pm 0.08$ | $-4.05 \pm 0.09$ | $-6.03 \pm 0.07$ |
| RSA | $-5.00 \pm 0.08$ | $-5.17 \pm 0.08$ | $-3.72 \pm 0.10$ | $-5.76 \pm 0.08$ |

[a] $M_V^{b,i} =$ (slope) $\times \log V_{HI}^c +$ (zero point), $M_V^{b,i} = m_V - A_V^b - A_V^i - \mu_0$.

We impose further criterion of inclination $i > 45°$ and having good H I line width data[1] for the Tully-Fisher analysis, and 16 galaxies are left. It is found that 15 of the 16 galaxies belong to the Virgo S Cloud (the region with $\delta > 10°.5$; see de Vaucouleurs & Corwin 1986). The distance of the S Cloud is claimed to be slightly smaller than the Virgo core (e.g., Fouqué et al. 1990). Accordingly, we use the 15 galaxies to determine the distance of the S Cloud. The correction of the difference of the distance between the S Cloud and the core of Virgo is shown in § B4.

The data for the 15 galaxies are shown in Table 7. The Galactic absorptions are taken from BH. As the Virgo Cluster is close to the north Galactic pole, the Galactic absorption given in RSA is zero. BH also give $A_V^b \sim 0$ for Virgo galaxies, while that given in RC2 is $\sim 0.15$ mag. We present the four estimates of internal absorption correction by the four prescriptions listed in Appendix A. We force the slope of the local calibrators onto the Virgo data and estimate the Virgo distance. The distance moduli of the Virgo based on the 12 combinations of Galactic and internal absorption corrections are summarized in Table 8.

### B2. THE INFLUENCE OF USING DIFFERENT CORRECTION METHODS FOR GALACTIC AND INTERNAL ABSORPTIONS

We examine the uncertainty of the Virgo distance due to the different correction methods of Galactic and internal absorptions. First, we find in Table 8 that the difference of the internal absorption correction hardly changes the Virgo distance. This is explained as follows: The amount of internal absorption correction to each galaxy type differs among the four methods by as much as $\sim 0.6$ mag. However, the difference of the *mean* amount of correction between the local calibrators and the Virgo galaxies is almost the same with different methods. Accordingly, the Virgo distance moduli are insensitive to the change of the method of internal absorption correction. This is rather fortuitous in the case of our Virgo sample, and it is noted that this is not always the case for samples of different morphological type mix. Second, it is found that the influence of the different Galactic absorption correction is also small. The disagreement of the Virgo distance moduli among the three methods is as small as 0.01 mag. Consequently, it is concluded that the uncertainty of the Virgo distance modulus due to the different correction methods for Galactic and internal absorptions is extremely small, at most 0.1 mag.

We take the estimates by BH as the reference values for Galactic absorptions. Averaging the four values corresponding to the four

[1] When a galaxy has more than one H I measurement, the mean value $\overline{V_{\rm H\,I}}$ is used. However, when the scatter around the mean value $\overline{V_{\rm H\,I}}$ is larger than $0.1\,\overline{V_{\rm H\,I}}$, the galaxy is discarded. We also reject NGC 4569 because it does not have sufficient H I gas (Guhathakurta et al. 1988).

TABLE 7

BASIC PARAMETERS OF THE VIRGO GALAXIES

| | | | | $A_V^i$ | | | | | |
|---|---|---|---|---|---|---|---|---|---|
| NAME (1) | TYPE (2) | $m_V$ (3) | $A_V^b$ (4) | TF85 (5) | RC2 (6) | RSA (7) | KW (8) | log $V_{\rm H\,I}^c$ (9) | $i$ (10) |
| NGC 4178..... | Sdm | 11.67 | 0.00 | 0.56 | 0.28 | 0.26 | 0.91 | 2.42 | 74 |
| NGC 4192..... | Sab | 10.28 | 0.11 | 0.72 | 0.35 | 1.00 | 0.50 | 2.64 | 80 |
| NGC 4212..... | Sbc | 11.33 | 0.06 | 0.30 | 0.11 | 0.33 | 0.46 | 2.50 | 51 |
| NGC 4216..... | Sb | 10.13 | 0.02 | 0.72 | 0.37 | 0.99 | 1.02 | 2.71 | 82 |
| NGC 4294..... | Scd | 12.26 | 0.02 | 0.45 | 0.22 | 0.45 | 0.75 | 2.32 | 67 |
| NGC 4298..... | Sc | 11.48 | 0.08 | 0.39 | 0.18 | 0.41 | 0.59 | 2.42 | 62 |
| NGC 4302..... | Sc | 11.46 | 0.05 | 0.72 | 0.36 | 0.65 | 1.02 | 2.54 | 81 |
| NGC 4383..... | Sa | 12.03 | 0.02 | 0.30 | 0.11 | 0.51 | 0.22 | 2.38 | 51 |
| NGC 4388..... | Sb | 11.14 | 0.08 | 0.72 | 0.36 | 1.00 | 1.02 | 2.54 | 81 |
| NGC 4450..... | Sab | 10.10 | 0.00 | 0.29 | 0.10 | 0.49 | 0.21 | 2.58 | 48 |
| NGC 4501..... | Sb | 9.62 | 0.07 | 0.40 | 0.19 | 0.64 | 0.61 | 2.75 | 64 |
| NGC 4595..... | Sb | 12.44 | 0.02 | 0.31 | 0.12 | 0.52 | 0.47 | 2.21 | 52 |
| NGC 4639..... | Sbc | 11.61 | 0.04 | 0.31 | 0.12 | 0.34 | 0.47 | 2.54 | 52 |
| NGC 4651..... | Sc | 10.78 | 0.02 | 0.38 | 0.18 | 0.40 | 0.58 | 2.60 | 61 |
| NGC 4654..... | Scd | 10.65 | 0.04 | 0.36 | 0.16 | 0.38 | 0.61 | 2.49 | 59 |

NOTES.—Col. (2): Morphological type taken from the PANBG. Col. (3): $V$ band apparent magnitude taken from the PANBG. Col. (4): Galactic absorption taken from BH. Cols. (5)–(8): Internal absorptions computed by the prescriptions TF85, RC2, RSA, and KW, respectively. Col. (9): Logarithm of corrected line width. Col. (10): Inclination.

TABLE 8

DISTANCE MODULI OF THE VIRGO S CLOUD FROM vTF RELATION BASED ON THE 12 COMBINATIONS OF DIFFERENT CORRECTION METHODS FOR GALACTIC AND INTERNAL ABSORPTIONS

| | $A_V^i$ | | | | |
|---|---|---|---|---|---|
| $A_V^b$ (1) | TF85 (2) | RC2 (3) | RSA (4) | KW (5) | MEAN (6)[a] |
| BH ..... | $31.13 \pm 0.13$ | $31.14 \pm 0.13$ | $31.14 \pm 0.15$ | $31.20 \pm 0.13$ | 31.15 |
| RC2 ..... | $31.12 \pm 0.12$ | $31.13 \pm 0.12$ | $31.13 \pm 0.14$ | $31.19 \pm 0.12$ | 31.14 |
| RSA ..... | $31.12 \pm 0.12$ | $31.13 \pm 0.12$ | $31.13 \pm 0.15$ | $31.20 \pm 0.12$ | 31.15 |

[a] Average of the four values corresponding to the four methods of internal absorption correction.

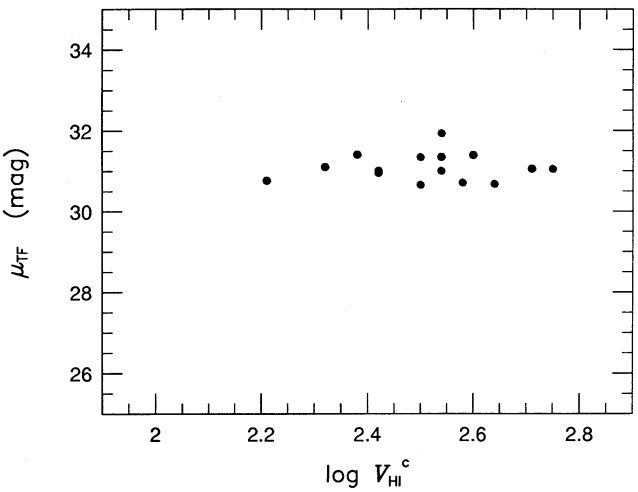


FIG. 9.—Distance moduli of the 15 galaxies in the Virgo S Cloud plotted against log $V_{H\,I}^{c}$. There is no trend that galaxies with smaller log $V_{H\,I}^{c}$ have smaller distance moduli.

methods of internal absorption correction, we obtain the Virgo distance modulus to be 31.15, 31.14, and 31.15 mag for BH, RC2, and for RSA. Our best estimate is then

$$\mu_{Vir} = 31.15^{+0.00}_{-0.01} \pm 0.15 \text{ (mag)} ,$$

where 0.15 mag is the root of the square sum of the two dispersions: one is the dispersion of the Virgo vTF relation (0.15 mag), and the other is the dispersion due to the difference of the method of internal absorption correction (0.03 mag).

### B3. THE INFLUENCE OF THE INCOMPLETENESS BIAS

The Virgo sample we use is a magnitude-limited sample (see PANBG). It is claimed that the straightforward fitting of the TF relation to a magnitude-limited sample of a cluster gives an erroneous distance (Teerikorpi 1987): For a magnitude-limited sample, the distance of a galaxy with smaller H I line width (hence fainter intrinsic luminosity) is smaller due to an observational limit imposed on the apparent magnitude and thus the cluster distance derived as the mean of the distances of the cluster members is smaller than the true value.

In order to examine this effect, we plot the distance moduli of the 15 Virgo galaxies against their H I line widths in Figure 9 (Galactic and internal absorption corrections are taken from BH and TF85, respectively). We find little trend that galaxies with smaller H I line widths give smaller distance moduli. Therefore, the effect of the sample incompleteness on the distance determination is negligible in our Virgo sample.

### B4. THE HUBBLE EXPANSION VELOCITY OF THE VIRGO CLUSTER

We use the Virgo Cluster as the reference cluster with the known Hubble expansion velocity. Aaronson et al. (1986) estimated $V_H^{Vir}$ to be 1342 km s$^{-1}$ combining the Virgo distance given in Aaronson et al. (1982) with the distance and recession velocity data of 10 distant clusters. We also adopt this value in the present study. However, the Virgo distance we estimated in the preceding subsection is in fact the distance of the S Cloud. Hence, when we use the value of 1342 km s$^{-1}$, we must correct the difference of the distance modulus between the S Cloud and the core of the Virgo Cluster, $\Delta\mu_{Vir}$. Distances of the 16 Virgo spirals, out of which 10 are in the S Cloud, are presented in Aaronson et al. (1982). Using these, we estimate $\Delta\mu_{Vir}$ to be 0.18 mag. The distance modulus of Virgo based on the K90 is, thus, $\mu_{Vir} = 31.33$ mag. The peculiar velocity of a galaxy is computed as

$$V_{pec} = V_{obs} - 1342 \times 10^{0.2(\mu_0 - 31.33)} \text{ (km s}^{-1}) ,$$

where $\mu_0$ is the distance modulus of the galaxy.

### B5. THE HUBBLE CONSTANT DERIVED FROM THE VIRGO CLUSTER

Finally, we estimate the Hubble constant $H_0$ using the Virgo distance. From the discussion above, the Virgo distance is

$$d_{Vir} = 10^{0.2(31.33 \pm 0.15) - 5.0}$$
$$= 18.5 \pm 1.3 \text{ (Mpc)} .$$

The Hubble constant is thus estimated to be

$$H_0 = 1342/d_{Vir}$$
$$= 73 \pm 5 \text{ (km s}^{-1} \text{ Mpc}^{-1}) .$$

The error includes only the internal error derived from our vTF relation of Virgo (see § B2). We think that the error in $V_H^{Vir}$ is small because $V_H^{Vir}$ is determned using the sufficiently distant clusters whose peculiar motions can be neglected. However, it should be noted that there remains as much as ~30% of discrepancy in the estimates of $d_{Vir}$ among astronomers.

REFERENCES


Aaronson, M., Bothun, G., Mould, J., Huchra, J., Schommer, R. A., & Cornell, M. E. 1986, ApJ, 302, 536
Aaronson, M., Huchra, J., & Mould, J. 1979, ApJ, 229, 1
———. 1980, ApJ, 237, 655
Aaronson, M., Huchra, J., Mould, J., Schechter, P. L., & Tully, B. R. 1982a, ApJ, 258, 64
Aaronson, M., et al. 1982b, ApJS, 50, 241 (A82G)
Abell, G. O. 1958, ApJS, 3, 211
Abell, G. O., Corwin, H. G., Jr., & Olowin, R. P. 1989, ApJS, 70, 1
Bertschinger, E., Dekel, A., Faber, S. M., Dressler, A., & Burstein, D. 1990, ApJ, 364, 370
Burstein, D., & Heiles, C. 1984, ApJS, 54, 33 (BH)
Collins, C. A., Joseph, R. D., & Robertson, N. A. 1986, Nature, 320, 506
Davis, M., & Peebles, P. J. E. 1983, ApJ, 267, 465
de Vaucouleurs, G. 1978, in IAU Symp. 79, The Large Scale Structure of the Universe, ed. M. S. Longair & J. Einasto (Dordrecht: Reidel), 205
de Vaucouleurs, G., & Bollinger, G. 1979, ApJ, 233, 433
de Vaucouleurs, G., & Corwin, H. G., Jr. 1986, AJ, 92, 722
de Vaucouleurs, G., de Vaucouleurs, A., & Corwin, H. G., Jr. 1976, Second Reference Catalogue of Bright Galaxies (Austin: Univ. of Texas Press) (RC2)
de Vaucouleurs, G., de Vaucouleurs, A., Corwin, H. G., Jr., Buta, R. J., Paturel, G., & Fouqué, P. 1991, Third Reference Catalogue of Bright Galaxies (New York: Springer-Verlag) (RC3)
Dressler, A. 1988, ApJ, 329, 519
Dressler, A., & Faber, S. M. 1990, ApJ, 354, 13
Dressler, A., Faber, S. M., Burstein, D., Davies, R. L., Lynden-Bell, D., Terlevich, R., & Wegner, G. 1987a, ApJ, 313, L37
Dressler, A., Faber, S. M., & Burstein, D. 1991, ApJ, 368, 54
Dressler, A., Lynden-Bell, D., Burstein, D., Davies, R. L., Faber, S. M., Terlevich, R., & Wegner, G. 1987b, ApJ, 313, 42
Faber, S. M., & Burstein, D. 1988, in Large-Scale Motions in the Universe, ed. V. C. Rubin & G. V. Coyne (Princeton: Princeton Univ. Press), 115 (FB)
Faber, S. M., Wegner, G., Burstein, D., Davies, R. L., Dressler, A., Lynden-Bell, D., & Terlevich, R. J. 1989, ApJS, 69, 763 (7S)
Fixen, D. J., Cheng, E. S., & Wilkinson, D. T. 1983, Phys. Rev. Lett., 50, 620
Fouqué, P., Bottinelli, L., Gouguenheim, L., & Paturel, G. 1990, ApJ, 349, 1
Freedman, W. L. 1990, ApJ, 355, L35
Fukugita, M., Okamura, S., Tarusawa, K., Rood, H. J., & Williams, B. A. 1991, ApJ, 376, 8
Guhathakurta, P., van Gorkom, J. H., Kotanyi, C. G., & Balkowski, C. 1988, AJ, 96, 851
Han, M., & Mould, J. 1990, ApJ, 360, 448
Huchtmeier, W. K., & Richter, O.-G. 1989, A General Catalog of H I Observations of Galaxies (New York: Springer-Verlag) (HR89)
Ichikawa, S., Okamura, S., Watanabe, M., Hamabe, M., Aoki, T., & Kodaira, K. 1987, Ann. Tokyo Astron. Obs., 21, 285
Kodaira, K., Okamura, S., & Ichikawa, S. 1990, Photometric Atlas of Northern Bright Galaxies (Tokyo: Univ. of Tokyo Press) (PANBG)
Kodaira, K., & Watanabe, M. 1988, AJ, 96, 1593 (KW)
Lubin, P. M., & Villela, T. 1986, in Galaxy Distances and Deviations from Universal Expansion, ed. B. F. Madore & R. B. Tully (Dordrecht: Reidel), 169
Lubin, P. M., Villela, M. P., Epstein, G. L., & Smoot, G. F. 1985, ApJ, 298, L1
Lynden-Bell, D., Faber, S. M., Burstein, D., Davies, R. L., Dressler, A., Terlevich, R. J., & Wegner, G. 1988, ApJ, 326, 19
Lynden-Bell, D., & Lahav, O. 1988, in Large-Scale Motions in the Universe, ed. V. C. Rubin & G. V. Coyne (Princeton: Princeton Univ. Press), 199
Malmquist, K. G. 1920, Medd. Lund Astron. Obs., Ser. 2., No. 22, 19
Mathewson, D. S., Ford, V. L., & Buchhorn, M. 1992, ApJ, 389, L5
Nilson, P. 1973, Uppsala General Catalogue of Galaxies (Uppsala Astr. Obs. Ann., Vol. 6) (UGC).
Peebles, P. J. E. 1988, ApJ, 332, 17
Pierce, M. J., & Tully, R. B. 1988, ApJ, 330, 579
Sandage, A., & Tammann, G. A. 1981, A Revised Shapley-Ames Catalog of Bright Galaxies (Washington D.C.: Carnegie Institution of Washington) (RSA)
Saunders, W., et al. 1991, Nature, 349, 32
Scaramella, R., Vettolani, G., & Zamorani, G. 1991, ApJ, 376, L1
Takase, B., Ichikawa, K., Shimizu, M., Maehara, H., Hamajima, K., Noguchi, T., & Ohashi, M. 1977, Ann. Tokyo. Astron. Obs., 16, 74
Tammann, G. A. 1987, in IAU Symp. 124, Observational Cosmology, ed. A. Hewitt & G. R. Burbidge (Dordrecht: Reidel), 151
Tammann, G. A., & Sandage, A. 1985, ApJ, 294, 81
Teerikorpi, P. 1987, A&A, 173, 39
Tonry, J. M., & Davis, M. 1981, ApJ, 246, 680
Tully, R. B. 1982, ApJ, 257, 389
Tully, R. B., & Fisher, J. R. 1977, A&A, 54, 661
———. 1987, Nearby Galaxies Atlas (New York: Cambridge Univ. Press)
Tully, R. B., & Fouqué, P. 1985, ApJS, 58, 67 (TF85)
Yahil, A. 1988, in Large-Scale Motions in the Universe, ed. V. C. Rubin & G. V. Coyne (Princeton: Princeton Univ. Press), 219
Yahil, A., Sandage, A., & Tammann, G. 1980, ApJ, 242, 448